Supplementary Information
(Control of ionization and dissociation by optical pulse trains)

A. Kirrander, Ch. Jungen, and H. H. Fielding

(Dated: January 9, 2010)

I. OVERVIEW

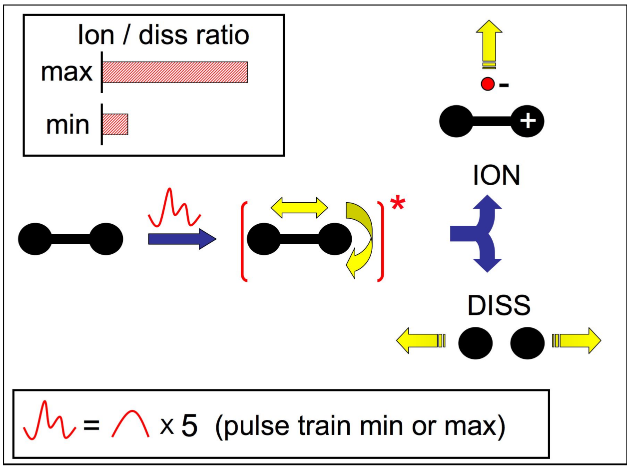

FIG. 1: Schematic (conceptual) representation of the physical processes simulated in the calculations. An H_2 molecule is electronically, vibrationally and rotationally excited by five laser pulses. By changing the time-delay between the pulses, the molecule can be pushed towards ionization (pulse train max) or dissociation (pulse train min), thereby changing the branching ratio between the two processes.

A schematic overview of the physical situation simulated in the calculations is shown in Figure 1. This supplement gives further information on the three topics in the appendix of the paper. Note that natural units for electron scattering are used throughout[1,2].

II. TIME-DEPENDENT MQDT

The molecular wave functions and dipole transition moments are calculated using MQDT, which renders N_o wave functions, one for each product channel, of the form

$$|\Psi_k^-(r,E)\rangle\rangle = \sum_{j=1}^{N_o+N_c} |j\rangle\phi_j(r,E)T_{kj}(E), \qquad (1)$$

where the sum runs over N_o+N_c open and closed channels, each channel corresponding to a specific state of the molecular ion and the outer electron. The kets $|j\rangle$ contain the electronic, vibrational and rotational state of the molecular ion, and the spin and angular momentum of the outer electron, whose energy normalized radial wave function is given by $\phi_j(r,E)$. The $N_o \times (N_o+N_c)$ expansion coefficients T_{kj} are calculated by MQDT such that the total wave functions $|\Psi_k^-(r,E)\rangle\rangle$ fulfill the appropriate boundary conditions at each energy[3]. The non-adiabatic interactions, included through a scattering matrix for the interaction between electron and molecular ion, mix the different channels and give a treatment similar to configuration interaction in *ab initio* theory[4]. Strictly speaking, the wave functions in Equation (1) are valid outside a radius r_c, corresponding to the radius of the ground state of the molecule, which is much more compact than the excited states. On the other hand, the dipole transition moments $D_k^-(E) = \langle s|r|\Psi_k^-\rangle$, where s denotes the molecular ground state, are determined inside the radius r_c. Dissociation channels, leading to neutral atoms on a specific adiabatic potential are included within the same framework[5].

The dynamics can be studied by the probability density, $\left|\langle j|\Psi_k^-(r,t)\rangle\right|^2$, giving the time-dependent population, $P_j(t)$, in each channel j,

$$P_j(t) = \int \left|\langle j|\Psi_k^-(r,t)\rangle\right|^2 \, dr. \qquad (2)$$

Alternatively, one can study the probability flux $\mathbf{j}$,

$$\mathbf{j} = \frac{1}{m_\mu}\mathrm{Im}\left[\langle\Psi_k^-(r,t)|j\rangle\frac{\partial}{\partial r}\langle j|\Psi_k^-(r,t)\rangle\right], \qquad (3)$$

where m_μ is the reduced mass in channel j. The final product cross sections, σ_k, in each product channel k are proportional to the square amplitude of the partial dipole transition moments and the spectral profile of the optical pulse,

$$\sigma_k = \int |\epsilon(E)|^2|D_k^-(E)|^2 \, dE. \qquad (4)$$

The partial product yields, $Y_k = \sigma_k/\sigma_{tot}$, are defined relative the total product cross section,

$$\sigma_{tot} = \sum_k^{N_o} \sigma_k, \qquad (5)$$

such that the total yield Y_{tot}=1.

The complex excitation function, $\mathbf{cef}(E,t)$, abbreviated CEF, appears in Equation (1) in the Appendix of the paper. It is defined[2,6] as,

$$\mathbf{cef}(E,t) = \int_{-\infty}^{\infty} dE' \, \epsilon(E') \int_{T=-\infty}^{t} dt' \, e^{\imath(E-E')t'}, \qquad (6)$$

where $\epsilon(E)$ is the Fourier transform of the time-dependent optical field $\epsilon(t)$. Essentially, Equation (6) shows the time-evolution of the spectral profile. At the end of the optical pulse, the integral over t' in Equation (6) becomes $2\pi\delta(E-E')$, making the CEF proportional to the Fourier transform of the optical pulse,

$$\mathbf{cef}(E, t\to\infty) = 2\pi\epsilon(E). \tag{7}$$

III. PULSE TRAINS

We are interested in a sequence of N identical and coherent pulses, $\epsilon_0(t)$, each centered at a different time t_i,

$$\epsilon(t) = \frac{1}{\sqrt{N}}\sum_{i=1}^{N}\epsilon_0(t-t_i), \tag{8}$$

where the normalization factor $1/\sqrt{N}$ ensures that the total excitation intensity of the pulse train is independent of the number of pulses. The time delay and relative optical phase between each pulse affects the interference of the excited wave packets dramatically. The asymptotic properties of the pulse train are given by the Fourier transform of the pulse train

$$\epsilon(E) = \frac{\epsilon_0(E)}{\sqrt{N}}\sum_{i=1}^{N}e^{\imath E t_i} = \frac{\epsilon_0(E)}{\sqrt{N}}F(E), \tag{9}$$

where $\epsilon_0(E)$ is the Fourier transform of a single pulse $\epsilon_0(t)$ and the net modulation of the pulse envelope resulting from the pulse train is contained in the function $F(E)$. This function provides a comb-like structure that modulates the single-pulse spectral profile $\epsilon_0(E)$; in the limit of a large number of pulses, we obtain a sharp frequency comb[7]. For a constant time delay $\triangle_0$ between pulses, $F(E)$ becomes a power series and can be summed analytically as,

$$F(E) = e^{\imath E\triangle_0(N-1)/2}\ \sin\frac{E\triangle_0 N}{2}\Big/\sin\frac{E\triangle_0}{2}, \tag{10}$$

which corresponds to a comb with narrow peaks of height N and width $2\pi/\triangle_0 N$, with each pair of peaks separated by $2\pi/\triangle_0$. By adjusting the number of pulses N and the time delay $\triangle_0$ between them, specific net optical pumping can be achieved.

This requires that we can align the comb with relevant spectral features of the molecule. To position a peak at a particular target energy E_f, the time delay $\triangle_0$ must be adjusted by a small amount $\gamma(E_f) \ll \triangle_0$,

$$\gamma(E_f) = -\frac{1}{E_f}\mathrm{mod}(E_f\triangle_0, 2\pi), \tag{11}$$

where we use the numerical modulo function, defined as $\mathrm{mod}(x,y) = x - \mathrm{floor}(\frac{x}{y})y$. Once a base position and spacing of the comb have been set, a full range of alignments can be explored by changing the relative optical phase θ between subsequent pulses. This amounts to small additional corrections in the time delay, rendering the final time delay

$$\triangle = \triangle_0 + \gamma(E_f) + \theta/E_0, \tag{12}$$

where E_0 is the central frequency of the optical pulses $\epsilon_0(t)$. One can expect the time delay $\triangle_0$ to be on the order of picoseconds, while the adjustments $\gamma(E_f)$ and θ/E_0 would be about two orders of magnitude shorter.

Numerically, we optimize the time-delay $\triangle$ directly. In general, the coarse time-delay $\triangle_0$ is found to be quite stable (or as here, constant), as it corresponds to some system-specific dynamics. On the other hand, the final outcome of the optimization is highly sensitive to the exact adjustments of the relative optical phase θ.

A. Gaussian pulses

In Equation (8), we make no assumption about the shape of the optical pulses $\epsilon_0(t)$, but in our calculations we use Gaussian pulses, which are easily generated experimentally and for which the CEF can be calculated analytically[2,6]. A single Gaussian optical pulse $\epsilon_g(t)$ can be written as

$$\epsilon_g(t) = \epsilon_t e^{-2\ln 2(t/\tau_t)^2}\left(e^{\imath E_0 t} + e^{-\imath E_0 t}\right), \tag{13}$$

where E_0 is the central optical frequency, ϵ_t the amplitude and τ_t the full width at half maximum (FWHM) pulse duration, defined for the *intensity* profile, proportional to the square modulus of the electric field. The frequency domain representation obtained by a Fourier transform of Equation (13) is

$$\epsilon_g(E) = \epsilon_E\left(e^{-\alpha^2(E-E_0)^2} + e^{-\alpha^2(E+E_0)^2}\right), \tag{14}$$

with $\epsilon_E = \epsilon_t\tau_t/\sqrt{4\ln 2}$ and $\alpha = \tau_t/\sqrt{8\ln 2}$. The (FWHM) width is $\tau_E = 4\ln 2/\tau_t$.

IV. CALCULATIONS

Dipole excitation of ground state H_2 molecules leads to singlet ungerade H_2 states (J=1, negative total parity) and is dominated by l=1 partial waves, as expected from single-photon selection rules. Calculated resonance positions for the three strongest resonances, n=34 and v=1,2, are given in Table I, along with the best available experimental positions and lifetimes etc. Note that the various intrinsic times of the system span almost three orders of magnitude.

Analysis of the wave function eigenvectors from the MQDT calculation allows us to identify the main components of the time-independent spectrum, as shown in

TABLE I: The three complex resonances (n=34 and v=1,2) in the calculated singlet ungerade H_2 spectrum. The integrated intensities for the three resonances are more than an order of magnitude stronger than all other resonances in this region of the spectrum. At energies below the resonance n=34, the integrated intensities are in the range 1.5–4.6$\times10^{-3}$, while at energies above the resonance v=1 they are in the range 1.3$\times10^{-3}$–1.1$\times10^{-4}$. In both cases the integrated intensities decrease away from the resonance. Also given are widths estimated from the calculated spectrum, along with corresponding lifetimes. The table gives characteristic time scales associated with the resonances: (i) the classical orbit period (Kepler) time $\tau_{\rm cl}(n) = 1.52\times10^{-4}n^3$ ps, and (ii) the times τ_{ij} associated with the quantum beats between the coherently excited resonances i and j.

	Approximate description	Calculated energy/cm^{-1}	Observed energy/cm^{-1}	Calculated width/cm^{-1}	Integrated intensity	Life time/ps	Kepler time/ps	Beat time/ps
n=34	$34p2,v^+$=0	124494.0	124495.5	1.7	3.3$\times10^{-2}$	3.2	6.0	$\tau_{34,2} \approx 16$
v=2	$5p\pi,v$=2	124496.4	124495.5	0.25	1.7$\times10^{-2}$	21.3	0.02	$\tau_{2,1} = 3.0$
v=1	$7p\pi,v$=1	124507.5	124507.2	0.06	1.2$\times10^{-2}$	83	0.05	$\tau_{1,34} = 2.6$

TABLE II: Channel groupings for population (probability) analysis of the ionization and dissociation dynamics. The calculation uses two open dissociation channels corresponding to molecular dissociation on the $B'^1\Sigma_u^+$ and $C^1\Pi_u$ states of H_2, and 20 $H_2^+(X^2\Sigma_g^+$, $v^+\geq0$, N^+=0,2) + e$^-$(l=1) channels.

Group	Comment	MQDT channel
Ion	Ionization	$H_2^+(v^+=0,N^+=0)$[a]
Diss	Dissociation	$B'^1\Sigma_u^+ \rightarrow$ H(1s)+H(n=2)
Ryd	Rydberg	$H_2^+(v^+=0,N^+=2)$[a]
$v=1$	interloper 1	$H_2^+(v^+=1,N^+=0$ and 2)[a]
$v=2$	interloper 2	$H_2^+(v^+=2,N^+=0$ and 2)[a]

[a] Plus electron $e^-(l=1)$. Electronic state of H_2^+ is $X^2\Sigma_g^+$.

TABLE III: Final product cross sections, σ_k, and branching ratios for the reference pulse and optimized pulse trains max and min. The time delays are defined according to Equation (12). The coarse time-delay is $\triangle_0$=2.99 ps and $\gamma(E_f$=124496 cm^{-1}) for both pulse trains, but the relative optical phase θ is different.

	reference	max	min
ion (σ_i)	1.40$\times10^{-3}$	4.11$\times10^{-3}$	3.26$\times10^{-4}$
diss (σ_d)	2.13$\times10^{-5}$	2.27$\times10^{-5}$	2.11$\times10^{-5}$
ratio (σ_i/σ_d)	66	181	15
phase (θ)	–	0.13π	0.75π

Figure 1 in the paper. These channels are presented in Table II.

To compare the yields between different excitation schemes, we normalize all cross sections by the total cross section, σ_{tot}, for the single reference pulse. Relative populations, useful to compare the dynamics for different excitation schemes side-by-side, are obtained by normalizing the populations $P_j(t)$ given by Equation (2) by the final product (ie. ionization or dissociation) cross section for each particular excitation scheme. Hence, relative population "1", corresponds to the final product cross section, σ_k, for that particular excitation scheme. See also text around Equations (4-5). The final product cross sections, σ_k, for the three excitation schemes are given in Table III.

---

[1] A. Kirrander and Ch. Jungen and H. H. Fielding, J. Phys. B **41**, 074022 (2008).

[2] A. Kirrander and H. H. Fielding and Ch. Jungen, J. Chem. Phys. **127**, 164301 (2007).

[3] F. Texier and C. Jungen, Phys. Rev. A **59**, 412 (1999).

[4] U. Fano, J. Opt. Soc. America **65**, 979 (1975).

[5] C. Jungen and S. C. Ross, Phys. Rev. A **55**, R2503 (1997).

[6] M. Shapiro and P. Brumer, *Principles of the Quantum Control of Molecular Processes*, ISBN 0-471-24184-9 (Wiley, 2003), 1st ed.

[7] S. T. Cundiff and J. Ye, Rev. Mod. Phys. **75**, 325 (2003).